DOI:10.1021/jf103083u

JOURNAL OF AGRICULTURAL AND FOOD CHEMISTRY
ARTICLE

Metabolites Involved in Oleuropein Accumulation and Degradation in Fruits of *Olea europaea* L.: Hojiblanca and Arbequina Varieties

Francisca Gutierrez-Rosales,[†] María Paz Romero,[‡] María Casanovas,[‡] María José Motilva,[‡] and María Isabel Mínguez-Mosquera*,[†]

[†]Grupo de Química y Bioquímica de Pigmentos, Departamento de Biotecnología de Alimentos, Instituto de la Grasa, Consejo Superior de Investigaciones Científicas (CSIC), Avenida Padre García Tejero, 4, 41012 Sevilla, Spain, and [‡]Food Technology Department, XaRTA-UTPV, Escuela Técnica Superior de Ingeniería Agraria, Universidad de Lleida, Alcalde Rovira Roure, 191, 25198 Lleida, Spain

The biosynthetic pathway of oleuropein (from 7-ketologanin, oleoside-11-methyl ester, 7-β-1-D-glucopyranosyl-11-methyl oleoside, and ligstroside to oleuropein) was investigated in two fruit species of Oleaceae, namely, Arbequina and Hojiblanca. Main oleuropein precursors and their metabolites, produced by the enzymatic hydrolysis mediated by β-glucosidase, were identified and quantified to establish the oleuropein transformation pathway. Changes in the concentration of these compounds were measured by direct control of *in vivo* fruit tissue during their ripening. High contents of aglycones at the initial stage of the process were caused by the high activity of β-glucosidase, which supports that oleuropein biosynthesis is coupled with enzymatic hydrolysis, producing its aglycone form. The low oleuropein content at this initial stage was caused by the imbalance between catabolic and anabolic pathways, favoring the former ones. Once the main polyphenol synthesis phase was completed, the biosynthetic capacity diminished and the content of all compounds decreased. Mass balance revealed that precursors of oleuropein, which are rapidly transformed by β-glucosidase and esterases, scarcely contributed to the accumulation of oleuropein. The biosynthetic pathway proposed by Damtoft applies for both varieties, but our study reveals that the β-glucosidase enzyme is involved in oleuropein synthesis. This enzyme shows high substrate specificity to oleuropein, which consequently is degraded to its aglycone form, with diminished efficacy of oleuropein biosynthesis. Different enzymatic activities of varieties will result in oleuropein accumulation and metabolic transformation of phenols.

KEYWORDS: Olive fruit; oleoside-11-methyl ester; ligstroside; tyrosol; oleuropein; aglycones; elenolic acid; metabolism; oleuropein precursors; β-glucosidase

INTRODUCTION

The nature of oleuropein biosynthesis in *Olea europaea* L. is complex and not yet well-understood. Type and quantity of polyphenols in olive tissues vary greatly depending upon variety, stage of ripening, and development and growing conditions. Elenolic acid glucoside and demethyloleuropein are glucosylated derivatives of oleuropein, which accumulate during ripening of olive (*O. europaea* L.) fruits. These compounds appear simultaneously with a drop in oleuropein content and an increase in esterase activity (*1*). This work also indicates that, as well as being formed by esterase action, it is possible that elenolic acid glucoside and demethyloleuropein can be intermediaries in oleuropein biosynthesis. Furthermore, these authors also show in a previous study (*2*) that small-fruit varieties are characterized by high oleuropein and low verbascoside levels, while large-fruit varieties show the opposite profile. Although implication of esterase enzymes on the phenolic transformation has been studied, these authors conclude that β-glucosidase also ought to play an important role in the metabolic changes of these compounds (*1*,*2*). There is some controversy when trying to assign oleuropein as the major constituent of olive pulp, because its concentration varies greatly among varieties (*3*−*7*). *O. europaea* L. metabolic studies concerning phenolic compounds have only focused on fruit pulp. Ryan et al. (*8*) have also paid attention to other tissues, such as leaves and seeds, to establish the phenolic metabolism of Hardy's Mammoth cultivar. However, there are still many questions about the sites of biosynthesis and mode of translocation of phenols between tissues in *O. europaea* L. that remain unanswered. It has been suggested that different tissues have different phenolic composition, and as such, the metabolism of each plant tissue is characteristic (*3*, *8*). Alternatively, these same authors show that metabolism of individual plant tissues is similar or that phenolic precursors are easily translocated between tissues for subsequent biosynthesis (*9*).

Use of radio-labeled precursors in metabolic studies is not entirely adequate because of unpredictable incorporation rates, but it remains one of the most routinely employed methods for elucidating biochemical pathways and metabolic functions within natural plants and fruits. Consequently, previous studies

*To whom correspondence should be addressed. Telephone: +34-954691054. Fax: +34-954691262. E-mail: minguez@cica.es.

 Published on Web 12/01/2010

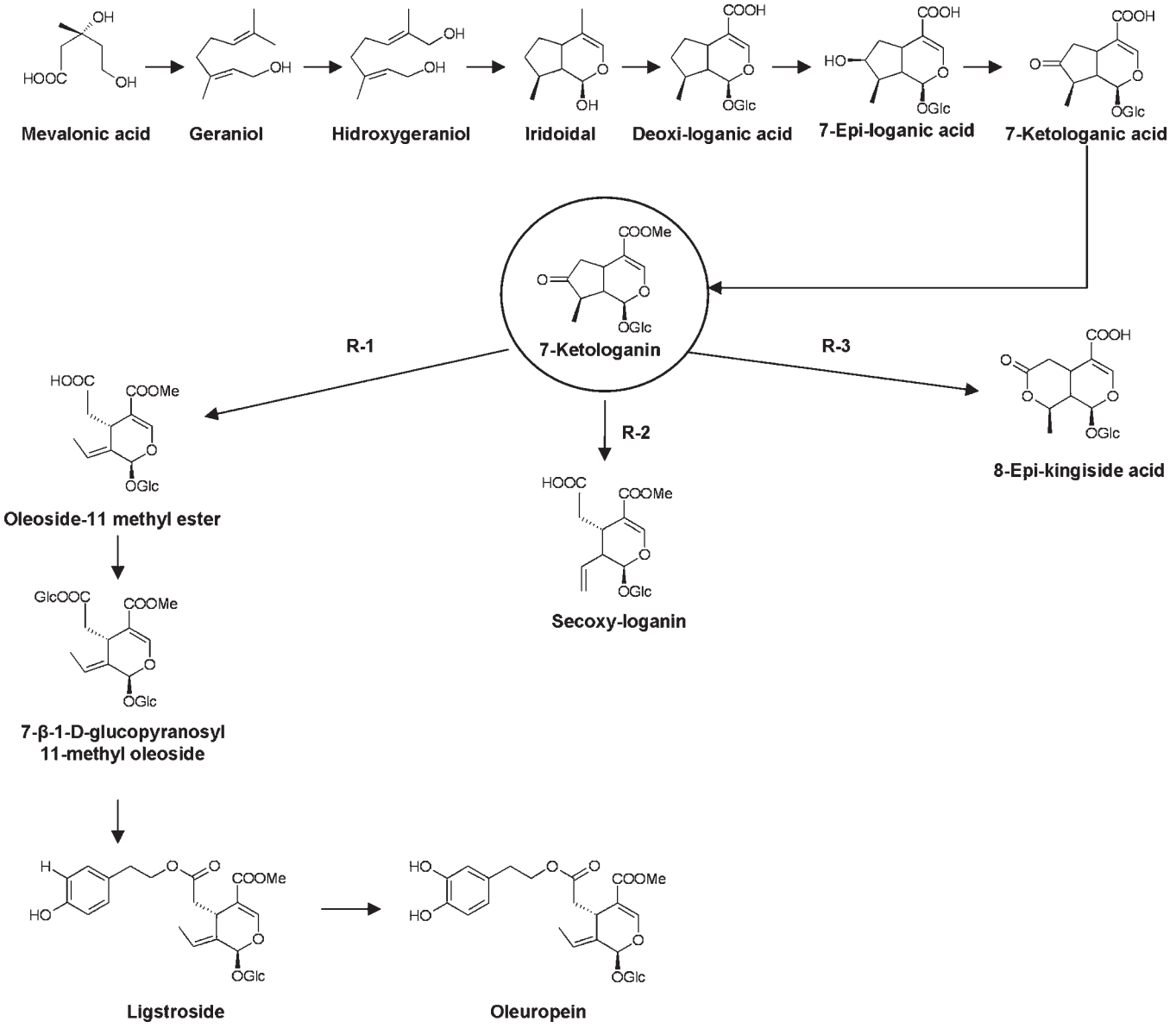

Figure 1. Biosynthesis route of oleuropein according to Damtoft et al. (*12*, *13*).

by Inouye et al. (*10*, *11*) on *O. europaea* L. were countered by Damtoft et al. because of the low incorporation percentage of the marker (*12*). Experiments on biosynthesis pathways in *O. europaea* L. are generally influenced by the fact that this species is a slow hydroponic absorber of water and that the presence of secoiridoids, causing extensive dispersion in the marker incorporation, is a common problem in Oleaceae family plants (*12*). With this in mind, these authors selected Oleaceae, which revealed acceptable water absorption levels (*13*) in subsequent studies.

These studies (*12*, *13*) show that the pathway to deoxyloganic acid, 7-epi-loganic acid, 7-ketologanic acid, and 7-ketologanin as last-stage carbocyclic iridoid precursors (**Figure 1**) could exist, although this sequence may vary among species and depending upon the season of the year. Analogues of 8-epi-kingisidic acid, kingisidic acid, secologanin, secoxyloganin, secologanoside, and oleoside-11-methyl ester were investigated in Fraxinus and Syringa as intermediates in the biosynthesis of 7-ketologanin and oleosides (*14*). None of the kingiside derivatives presented important incorporations, and in all cases, a high percentage of the precursor was re-isolated. Significant incorporation of oleoside-11-methyl ester into all iridoids with the exception of secologanoside and 8-epi-kingiside was observed. The accumulated incorporation was 19%, indicating that oleoside-11-methyl ester is a major participant in oleoside biosynthesis (**Figure 1**). The results also indicate that 7-ketologanin is the immediate precursor for oleoside-11-methyl ester.

These authors have tested possible secoiridoid intermediates, including 7-ketologanin and oleoside-11-methyl ester, the compound from which oleuropein (*13*) and similar iridoids in the Oleaceae family are derived. However, even in plant species selected by their high biosynthetic ability, neither intermediates of kingiside type nor secologanin type are incorporated to the expected degree for a true intermediate between 7-ketologanin and oleoside-11-methyl ester. These authors conclude that 7-ketologanin is the immediate precursor for oleoside-11-methyl ester, and this indicates that the conversion is most likely a single-step reaction (*13*) through a Baeyer−Villiger-type intermediate and that up to three different processes might be feasible (**Figure 1**). A reaction (R-1) initiated by rupture of the peroxide bond followed by cleavage of the C7−C8 bond and simultaneous abstraction of H9 would give rise to oleoside-11-methyl ester. A similar reaction (R-2) with abstraction of a proton from C10 would produce

secoxyloganin. Finally, 8-epi-kingiside acid and related compounds (R-3) could be formed via an alkyl shift of C8. Such a mechanism could explain the presence of the other iridoid products found with oleosides.

Considering that any isolated compound is apparently produced between 7-ketologanin and oleoside-11-methyl ester, apparently the biosynthesis of the oleosides is analogous to that presently accepted for the conversion of loganin to secologanin and related compounds, the so-called "ordinary" secoiridoids. Both reactions include oxidative ring fission, but the pathway to the oleosides starts at a higher oxidation level. Consequently, the products are also more highly oxidized (*13*). After 1 day, significant incorporations of the oleoside-11-methyl ester into 7-β-1-D-glucopyranosyl-11-methyl oleoside and ligstroside were detected in Syringa species, but only a small amount was incorporated into oleuropein (*12*, *14*). After 2 days, the same pattern prevailed, but the incorporation into oleuropein increased and was the highest observed after 3 days. This fact points to a rather slow biosynthetic conversion, which may be limited by the transport of the precursors within the plant. It also seems likely that oleuropein is formed from ligstroside by hydroxylation of the tyrosol moiety as a final step, and by inference, biosynthesis of oleuropein requires tyrosol and not hydroxytyrosol (*12*). This is supported by hydroponic feeding experiments with labeled deoxyloganic acid that show enrichment of ligstroside at about 4-fold that of oleuropein (*5*). From these results, the final steps in oleoside synthesis can be inferred as the direct conversion of 7-ketologanin to oleoside-11-methyl ester, followed by conversion to 7-β-1-D-glucopyranosyl-11-methyl oleoside, which originates ligstroside by esterification with tyrosol, and finally by hydroxylation, oleuropein (**Figure 1**).

The aim of this study was to determine metabolic changes occurring in the phenolic composition of olive pulp of Hojiblanca and Arbequina varieties involved in the oleuropein accumulation and degradation during growing, development, and ripening of the olive fruits. Oleuropein metabolism was followed considering the metabolites and pathway proposed by Damtoft et al. (*12*, *13*). Research conducted by Ryan et al. (*9*) has also been taken into account, as well as the reviews published by Ryan et al. (*5*), Pérez et al. (*15*), and Soler-Rivas et al. (*16*), in which all pathways match Damtoft's proposal. Involvement of the enzyme β-glucosidase was studied to correlate the evolution of the enzyme activity during the vegetative cycle of the fruits with oleuropein catabolism. For this objective, mass balance was performed, by monitoring the formation and transformation of the phenols included in the Damtoft-proposed pathway, considering the glucoside compounds, which can be β-glucosidase enzyme substrates.

MATERIALS AND METHODS

Raw Material. The study was carried out with selected fruits of the varieties Hojiblanca and Arbequina (*O. europaea* L.). Hojiblanca and Arbequina specimens were grown in an experimental agriculture station (Cabra, Spain), and five trees for each variety were selected. The experiment started 1 month after blooming, in the second week of June. The samples were harvested regularly every 15 days until December 15. For each sample, about 500 g of fruits was collected from olive trees of each variety. Samples were hand-picked between 10 a.m. and 11 a.m. A total of 13 samples were collected for each variety. For each ripening stage controlled in this study, a representative sample of 100 fruits was chosen as a function of their weight and color.

Chemicals and Reagents. High-performance liquid chromatography (HPLC)-grade ethanol was purchased from Romil Chemical Ltd. (Heidelberg, Germany), and *n*-hexane HPLC was purchased from Prolab (Leuven, Belgium). Standard *p*-hydroxy phenyl acetic acid was purchased from Sigma-Aldrich St. Louis, MO. For HPLC analysis, standards of tyrosol, hydroxytyrosol, and oleuropein were purchased from Extrasynthese (Genay, France). 3,4-DHPEA-EDA (dialdehydic form of elenolic acid linked to hydroxytyrosol), *p*-HPEA-EDA (dialdehydic form of elenolic acid linked to tyrosol), 3,4-DHPEA-EA (oleuropein aglycone), and *p*-HPEA-EA (aldehydic form of elenolic acid linked to tyrosol) were isolated by a semi-preparative HPLC method (*17*). Standard stock solutions of each compound were prepared in methanol. All of the solutions were stored in a dark flask at 4 °C. A standard solution of the phenolic compounds was prepared weekly at a concentration of 50 mg/L. A solution containing *p*-hydroxyphenylacetic acid [internal standard (IS)] at 150 mg/L was prepared. Methanol (HPLC supragradient grade) and formic acid were all provided by Scharlau Chemie (Barcelona, Spain). Water was of Milli-Q quality (Millipore Corp., Bedford, MA). Sodium borate, ethylenediaminetetraacetic acid (EDTA), phenylmethylsulfonyl fluoride (PMSF), dithiothreitol (DTT), polyvinylpolypyrrolidone (PVPP), and *p*-nitrophenyl-β-D-glucopyranoside (pNPG) were purchased from Sigma-Aldrich (St. Louis, MO).

Extraction of Phenolic Compounds. The methodology used for preparation of the lyophilized pulp was as follows: Immediately after harvesting, the olive pulp was cut into pieces of ca. 8−9 mm and frozen with liquid nitrogen. Then, the frozen pieces were kept at −32 °C before freeze drying. The freeze-drying process was performed in a Heto-FD3 freeze drier (Allerod, Denmark) at −54 °C and 0.066 mmHg for at least 48 h. The end of drying was considered when the weight of samples became constant.

Extraction of phenolic compounds from the lyophilized pulp was carried out following the method proposed by Ríos and Gutiérrez-Rosales (*18*). In summary, this consisted of adding 15 mL of an ethanol/water mixture (80:20, v/v) and 1 mL of IS solution to 1 g of lyophilized pulp. It was homogenized with an Ultra-Turrax blender for 4 min at 9500 rpm and at a low temperature (0−4 °C). The extract obtained was centrifuged at 0 °C for 15 min at 15 000 rpm and then vacuum-filtered. Any residual ethanol was removed by evaporation. The aqueous extract was rinsed with *n*-hexane to eliminate lipids and pigments. The *n*-hexane was subsequently removed, and the solution was made up to a final volume of 25 mL by adding the water/methanol mixture (70:30, v/v). The samples were stored in liquid nitrogen until they were analyzed.

Identification and Quantification of Phenols by HPLC−Electrospray Ionization (ESI)−Tandem Mass Spectrometry (MS/MS). The HPLC analysis of phenolic extracts was performed using a Waters AcQuity liquid chromatography system (Waters, Milford MA), equipped with a binary pump system (Waters, Milford, MA). The column was a SunFire C_{18} (4.5 × 150 mm, 3.5 μm) also from Waters. During the analysis, the column was kept at 30 °C and the flow rate was 0.8 mL/min. The mobile phase was water/formic acid (100:0.1, v/v) as eluent A and methanol as eluent B. The elution started at 10% eluent B, linearly increased to 55% eluent B in 45 min, further increased to 100% eluent B in 0.1 min. Then, it was kept isocratic for 9.9 min and back to initial conditions for 5 min. The re-equilibration time was 5 min. The injected volume was 10 μL, and all of the samples were filtered through 0.22 μm polyvinyldiene fluoride (PVDF) membrane (Tecknokroma, Barcelona, Spain) before the chromatographic analyses.

The HPLC was coupled to a photodiode array (PDA) detector AcQuity UPLC and a tandem quadrupole detector (TQD) mass spectrometer (Waters, Milford, MA). The wavelengths in the PDA detector were set at 278 and 339 nm. The MS/MS analyses were carried out on a TQD equipped with a Z-spray electrospray interface. The analyses were performed in negative mode, and the data were acquired in selected reaction monitoring (SRM). The ionization source working conditions were as follows: capillary voltage, 3 kV; source temperature, 150 °C; cone gas flow rate, 80 L/h; desolvation gas flow rate, 800 L/h; and desolvation temperature, 400 °C. Nitrogen (> 99% purity) and argon (99% purity) were used as nebulizing and collision gases, respectively. Cone voltages and collision energies were optimized by infusion of a standard solution of 10 mg/L of each analyzed compound in a mixture of methanol/water (50:50, v/v) at a flow rate of 10 μL/min. First, full-scan spectra were acquired to select the most abundant m/z value, and the cone voltage was optimized. In all cases, $[M - H]^-$ ions were found to be the most abundant. These ions were selected as the precursor ions, and afterward, the collision energies were studied to find the most abundant product ions. Therefore, the most sensitive transition was selected for quantification purposes, and the second transition was selected for confirmation. **Table 1** shows the

Table 1. Optimized SRM Conditions for the Analysis of Phenolic Compounds by HPLC−ESI−MS/MS

		quantification			confirmation		
compound	precursor ion (*m*/*z*)	product ion	cone voltage (V)	collision energy (eV)	product ion	cone voltage (V)	collision energy (eV)
p-hydroxyphenylacetic acid	151	107	20	10			
tyrosol	137	106	40	15	119	40	15
3,4-DHPEA-EDA	319	195	40	5	183	40	10
3,4-DHPEA-EA	377	275	35	10	307	35	10
p-HPEA-EDA	303	285	30	5	179	30	5
p-HPEA-EA	361	291	30	10	259	30	10
ligstroside	523	361	35	15	161	35	15
oleuropein	539	377	35	15	275	35	20
elenolic acid	241	139	30	15	165	30	10
oleoside-11-methylester	403	179	35	10	241	35	10
7-ketologanin	387	225	40	10	197	40	10
7-β-1-D-glucopiranosyl 11-methyl oleoside	567	405	40	15	507	40	10

MS/MS transitions for quantification and confirmation as well as cone voltage and collision energy values optimized for each of the analyzed compounds. Data acquisition was carried out by MassLynx software, version 4.1 (*19*).

The calibration curve (on the basis of the peak area or abundance) was plotted using $y = a + bx$, where y is the (oleuropein/IS) peak abundance ratio and x is the oleuropein concentration. Concentrations of the phenolic compounds were calculated by interpolating their (analyte/IS) peak abundance ratios on the calibration curve of oleuropein. The calibration curve was obtained by analyzing five different concentration levels. Three oleuropein solutions were prepared for each concentration. *p*-Hydroxyphenylacetic acid was used as an internal standard (IS) for the quantification. Secoiridoids were expressed as oleuropein. To perform the mass balance and normalize data, for each individual compound, the results were expressed as μmol/g of fruit.

Extraction and Measurement of β-Glucosidase Activity. The method proposed by Romero-Segura et al. (*20*) with slight modifications was used to determine β-glucosidase activity, and the method use for preparing acetonic powder was that proposed by Minguez-Mosquera et al. (*21*).

Preparation of the Protein Precipitate. The pitted and sliced fruits (25 g) were triturated with 20 volumes of acetone at −20 °C (500 mL). After maceration for 15 min in a freezer at −20 °C, the supernatant was removed by decantation and the residue was treated again with 8 volumes of acetone (200 mL). The operation was repeated until the supernatant was colorless (generally 4 washes were sufficient). Finally, the precipitate was collected by vacuum filtration and left to dry at ambient temperature. From each gram of fruit, approximately 0.12 g of powder was obtained.

Extraction of the Enzyme from the Protein Precipitate. The enzymatic activity was tested using pNPG as a substrate. The analysis was performed as follows: To obtain the raw extract, 0.25 g of powder was weighed and 17.5 mL of 0.1 mol/L borate buffer (pH 9), containing 5 mmol/L EDTA, 0.25% DTT (w/v), and 1 mmol/L PMSF, was added to it. Raw extract (100 μL) was added to 1 mL of phosphate buffer solution (pH 5.5) with 50 and 15 mmol/L pNPG. The absorbance of *p*-nitrophenol released at 405 nm at 50 °C was measured; this reflects the increase in the amount of *p*-nitrophenol released from pNPG. The concentration of the product was determined by calculating the molar extinction coefficient for pNPG (ε). The value for ε (630.8 M^{-1} cm^{-1}) was calculated from the absorbance measurements at different pNPG concentrations. The results are expressed in μKat/g of acetonic powder.

Statistical Analysis. Data in the text are mean values. Analysis of variance (ANOVA) for comparisons and the identification of significant differences between results were performed by applying the Tukey test. The level of statistical significance was set at $p < 0.05$. STATISTICA computer software (version 6.0, Statsoft, Tulsa, OK) was used in the statistical analysis of results.

RESULTS AND DISCUSSION

Fruit Development and Seasonal Changes in Moisture Content. **Figure 2** shows changes in the moisture content and weight of the fruit and stone, as a function of the harvesting date. Evolution of these parameters was used to establish three ripening stages, depending upon the weight increase, moisture, and fruit color. The first ripening stage corresponds to immature green fruit (intense green) of the Hojiblanca variety (from June 30 to August 28) and the Arbequina variety (from June 30 to September 8). The second ripening stage corresponds to green maturation (light green color) of the Hojiblanca variety (until November 17) and the Arbequina variety (until November 3). In the third stage, black maturation, fruits contain anthocyanins and may be mottled, purple, or black in color.

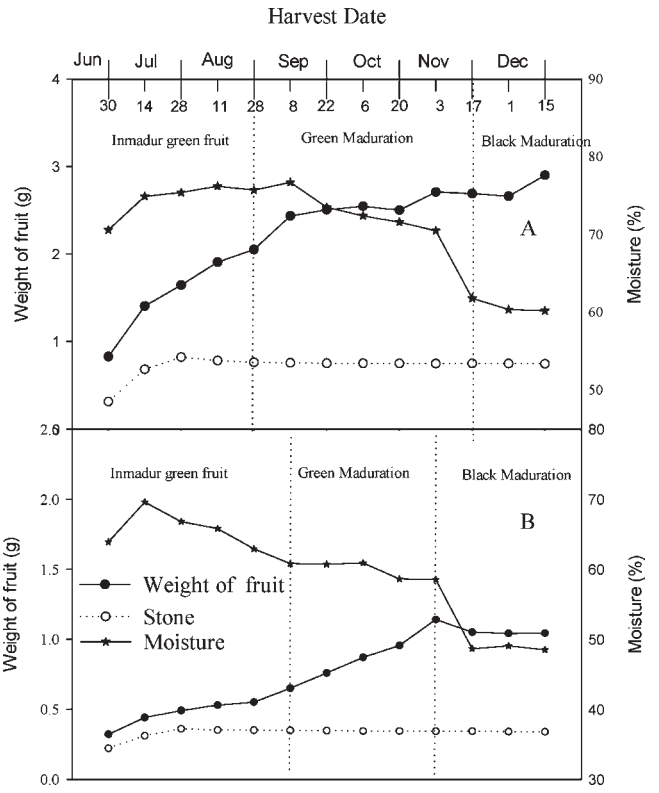

Figure 2. Changes in the weight of the fruit and stone (g) and moisture content (%) during different stages of ripening of (A) Hojiblanca and (B) Arbequina cvs.

The moisture percentage was always higher for Hojiblanca than Arbequina throughout the complete study. For the first Hojiblanca sampling, it was 70% and for the first Arbequina sampling, it was 63.9%, decreasing in both varieties to reach final

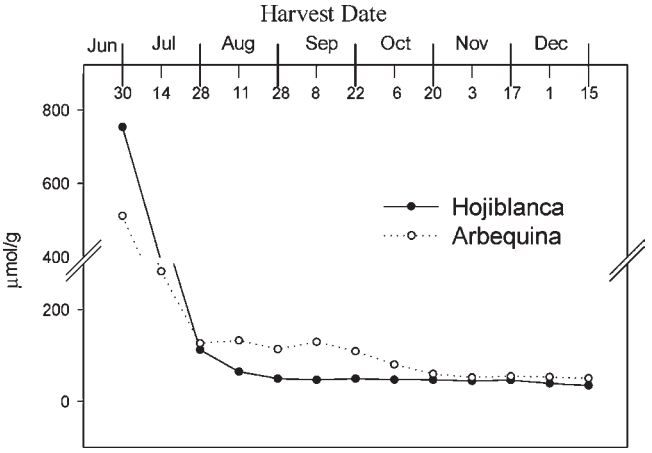

Figure 3. Changes in total phenol content during the vegetative cycle of the fruits (μmol/g of dry pulp) of the Hojiblanca and Arbequina cvs. Each value represents the mean ± relative standard deviation (RSD). RSD < 10%.

values of 60% for Hojiblanca and 48% for Arbequina. The weight of both stones and fruits was always lower for the Arbequina variety than Hojiblanca. For both varieties, the stone grew rapidly during the three initial harvestings and then immediately stabilized until the end of the experiment. Fruits of Hojiblanca variety quickly increased in weight in the immature green stage from 0.83 to 2 g at the end of that phase (August 28). Afterward, it continued to grow slowly during green and black maturation stages, reaching a weight of 3 g. The Arbequina variety fruits grew slowly in the immature fruit with a lower fruit weight value of 0.32 g. The fruits increased in weight until the end of green maturation (November 3), reaching 1.14 g. At this point, the weight stabilized and even decreased slightly during the black maturation stage.

Metabolic Changes during the Accumulation and Degradation of Oleuropein and the Role of β-Glucosidase. Figure 3 shows the changes in the total phenol content. The initial tendency in both varieties was a sharp decrease in the phenol concentration to reach low values even before the first ripening stage (immature green) finished (July 28). Thus, for the Hojiblanca variety, the change in content was from 753.7 to 112.2 μmol/g (85% decrease), and for the Arbequina variety, the change was from 511.6 to 126.2 μmol/g (75.3% decrease). After this sampling, the total phenol content showed minimal decreases and even kept constant until the end of the study, with the fruits of the Arbequina variety showing higher total phenol content in comparison to the values corresponding to the Hojiblanca variety. **Figure 4** shows the evolution of the fruit content (expressed in μmol/g of fruit) in phenols involved in oleuropein metabolism, including the precursors oleoside-11-methyl ester, tyrosol, ligstroside + iso-ligstroside, oleuropein + oleuroside, and the enzymatic products, derived from β-glucosidase activity, elenolic acid, oleuropein aglycone (3,4-DHPEA-EA), its dialdehyde form (3,4-DHPEA-EDA), and the aglycones corresponding to ligstroside (*p*-HPEA-EA and *p*-HPEA-EDA), for the Hojiblanca and Arbequina varieties. **Figure 5** depicts the proposed anabolic and catabolic pathways of oleuropein biosynthesis in accordance with the results from this study.

In accordance with the most accepted pathway for oleuropein synthesis proposed by Damtoft et al. (*12*, *13*), this compound is produced from the oleoside-11-methyl ester through the mediation of 7-ketologanin, which is derived from the deoxyloganic acid pathway (**Figure 1**). Oleoside-11-methyl ester is converted by glucosylation into 7-β-1-D-glucopyranosyl-11-methyl oleoside, which produces ligstroside after its esterification with tyrosol. This ester is hydroxylated to form oleuropein (**Figure 1**). Precursors, 7-ketologanin and 7-β-1-D-glucopyranosyl-11-methyl oleoside, were identified in this study, but we were unable to quantify them because their concentrations were under the detection limits, according to the linear calibration for measuring oleuropein. However, it was possible to perform a mass balance among both the precursors and enzymatic degradation products of oleuropein, coupling increases and decreases in the content of those phenolic compounds (**Figure 4**) and the scheme represented in **Figure 5**, as showed below.

Hojiblanca Variety. The highest Hojiblanca concentration values for the phenols measured in this study were obtained at the first sampling in the immature green stage, except for values corresponding to oleuropein + oleuroside and elenolic acid, which showed their highest content in the second sampling, also in the immature green stage. After that date (July 14), all of the compounds, except tyrosol, showed a sharp decrease (**Figure 4**). The trend of the fruit content on oleuropein precursors, oleoside-11-methyl ester, tyrosol, and ligstroside, was a decrease, which fits with the increase in the oleuropein content that rapidly decreased to reach the same plateau together with the rest of the phenols. This plateau remained constant during a significant part of the study. This evolution shows that the active phenol synthesis takes place in only young fruits. Only evolution of the tyrosol content showed some phases with increases, but the initial content values were not recovered in any case.

Figure 6A shows changes in β-glucosidase activity of fruits of the Hojiblanca variety throughout the study. This enzyme hydrolyses oleuropein and ligstroside to form the corresponding aglycones. The activity only reached values close to 0 during the green maturation stage, while in the rest of the sampling, the activity was always present. During the immature green stage, the activity showed a rise to reach the highest activity value (July 28). It was possible to detect a second rise after the lower levels were detected during the green maturation stage. Detection of the highest β-glucosidase at the initial ripening stage supports the appearance of high contents in the aglycone forms of oleuropein. The high endogenous activity by β-glucosidase and the great substrate affinity by oleuropein (*20*, *22*) detach the oleuropein synthesis from the ripening stages established in the study. Probably the maximum oleuropein content could have been reached at an earlier ripening stage not measured in the present study, and *in vivo* oleuropein synthesis is coupled with enzymatic hydrolysis to aglycone forms. Consequently, the high levels of oleuropein aglycone (3,4-DHPEA-EA) and its dialdehydic form (3,4-DHPEA-EDA) (**Tables 2** and **3**) could be formed through oleuropein via β-glucosidase activity. Similarly, the rapid decrease in the ligstroside content (from 125 to 3.7 μmol/g) to produce the corresponding aglycones could take place via β-glucosidase. The high initial catabolic activity would explain the low levels obtained for oleuropein with respect to the net initial formation of 3,4-DHPEA-EA (201.1 μmol/g) and 3,4-DHPEA-EDA (227.9 μmol/g) forms. Elenolic acid would be formed from oleoside-11-methyl ester by the intervention of β-glucosidase activity (*23*) (**Figure 5**).

β-Glucosidase is involved in several key points of the anabolic and catabolic routes of oleuropein biosynthesis, and as a consequence of the high activity observed during the immature stage, the catabolic pathway is more active than the anabolic pathway, limiting the efficacy of the oleuropein synthesis. Once the massive phase of polyphenol synthesis is complete, the biosynthetic capacity diminishes and there is a sudden decrease in all of the compound levels. This can be observed in **Figure 4**. The sharp drop in the concentration of the phenols involved in the oleuropein metabolism appears to indicate that there is a general decay of phenol biosynthesis, because no net increases were observed in

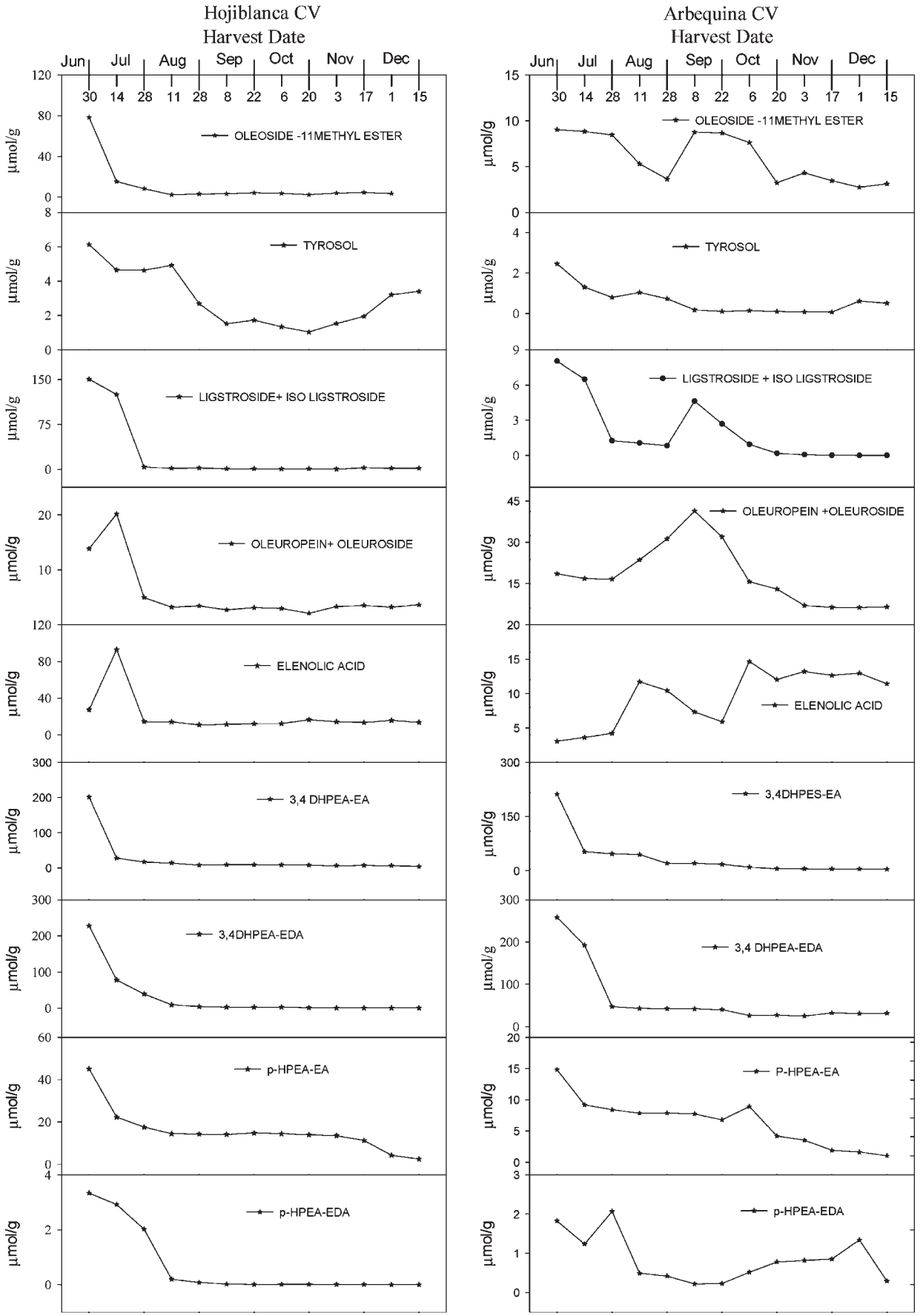

Figure 4. Changes in the concentration of polyphenols (μmol/g of dry pulp) integrated in the synthesis and degradation routes of oleuropein during the vegetative cycle of fruits of the Hojiblanca and Arbequina cvs. Each value represents the mean ± RSD. RSD < 10%.

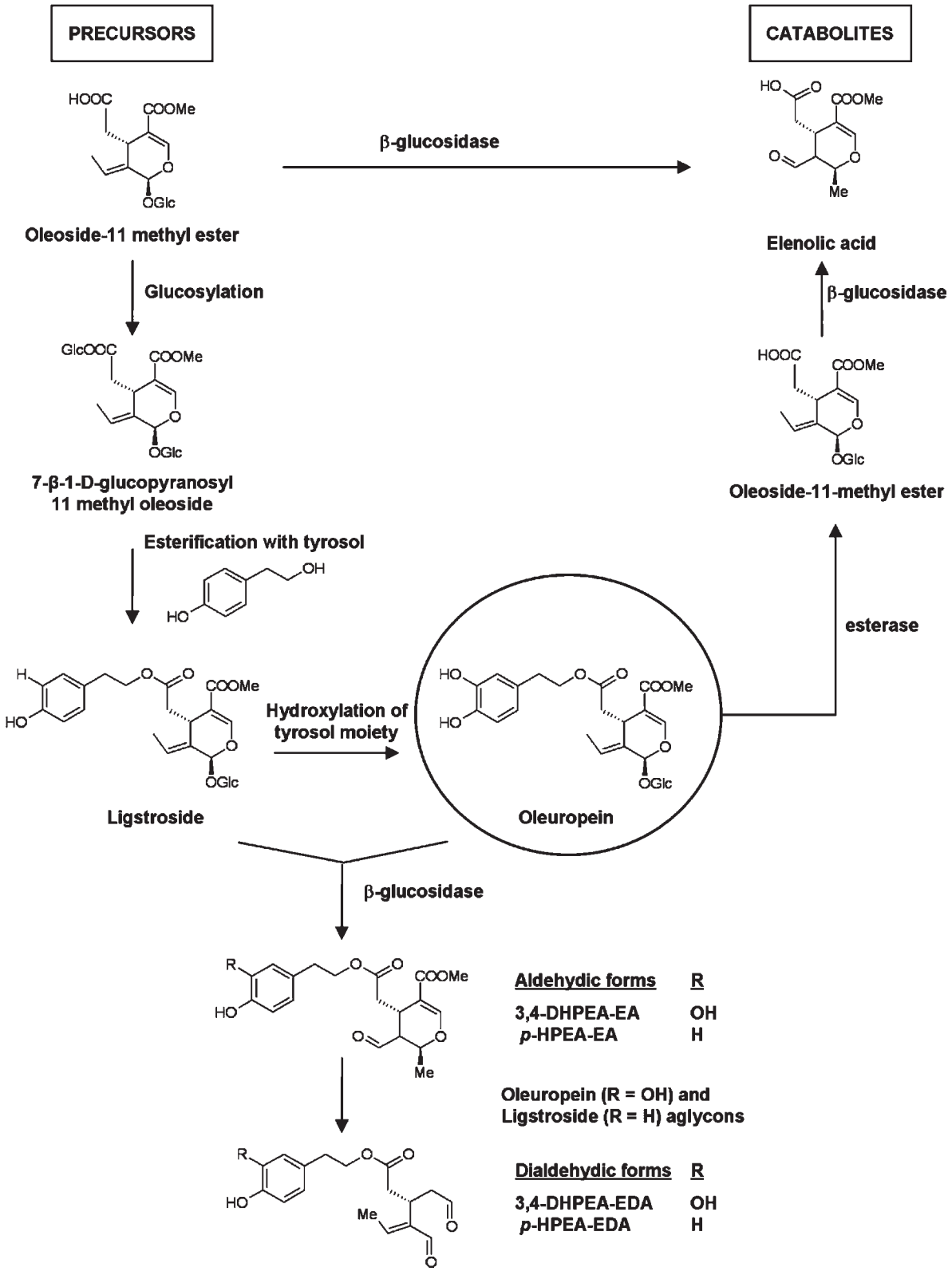

Figure 5. Proposed reactions for the implication of β-glucosidase on oleuropein metabolism in olive fruits (*O. europaea*) from the Hojiblanca and Arbequina cvs.

the concentrations of either precursors or catabolites (with the exception of tyrosol already mentioned). Thus, the decrease in the concentration of oleoside-11-methyl ester, which changed from 78.2 to 15.3 μmol/g, corresponds to an increase in the concentration of elenolic acid from 27.3 to 92.9 μmol/g. Consequently, oleoside-11-methyl ester would produce elenolic acid as a result of β-glucosidase activity (**Figure 6**). Tyrosol could be incorporated to the oleuropein synthesis. In fact, the tyrosol content changed from 6.1 to 4.6 μmol/g. This could have been used in the biosynthetic reactions, which transform oleoside-11-methyl ester in ligstroside after 7-β-1-D-glucopyranosil-11-methyl oleoside esterification with tyrosol. Thus, the initial tyrosol content of 6.1 μmol/g is incorporated to the oleuropein pathway, producing an increase of 6.3 μmol/g of oleuropein.

As described previously, the initial decrease in the number of phenols equals a total of 85% (**Figure 3**), which consequently

causes a generalized drop in all phenols. Consequently, the sharp decrease in the aglycone content indicates that aglycones are mobilized into other anabolic routes to produce other biosynthetic intermediates not considered in this study. Additionally, the results supports that oleuropein synthesis can be found in olive pulp and that it is produced according to the last phase of the Damtoft pathway (**Figure 1**), from ligstroside via oleoside-11-methyl ester, the main precursor, but synthesis is highly dependent upon alternative enzymatic processes involving β-glucosidase and esterase (**Figure 5**), which significantly modify the yield of the oleuropein synthesis.

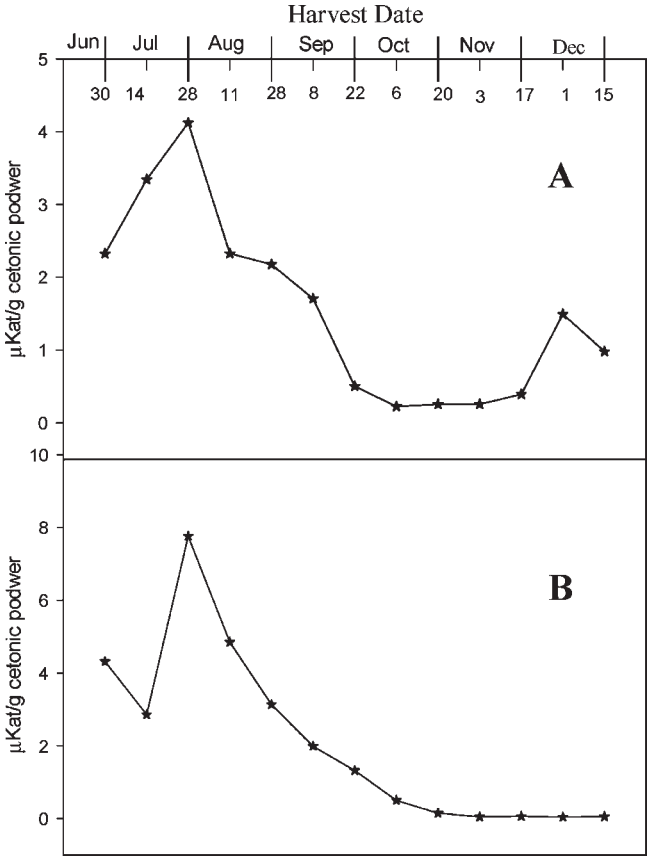

Figure 6. Changes in β-glucosidase during the vegetative cycle of the fruit (μKat/g of acetonic powder) of the (A) Hojiblanca and (B) Arbequina cvs. Each value represents the mean ± RSD. RSD < 5%.

Finally, to ascertain hypotheses concerning the role of 3,4-DHPEA-EDA and oleoside-11-methyl ester as the precursor and degradation product, respectively, of oleuropein, a look on the mass balances of those compounds could help to accept or disregard those roles. Several authors (*22*−*25*) suggest that 3,4-DHPEA-EDA formation involves a pathway that would include the transformation of the aldehydic form (3,4-DHPEA-EA) by opening the elenolic ring and successive isomerization of elenolic species to produce the dialdehydic structure, via decarboxylation. However, Ryan et al. (*8*, *9*) proposed that 3,4-DHPEA-EDA develops a precursor function of oleuropein and last of oleuroside, although they noted that rigorous research using markers is required to confirm this hypothesis. Taking into account our results, if 3,4-DHPEA-EDA functions as a precursor of oleuropein through the mediation of aglycone, the drastic decrease in 3,4-DHPEA-EDA would have produced a significant increase in oleuropein. It can be established that the dialdehydic form does not play any role as a precursor of oleuropein, as suggested by Ryan et al. (*9*) (**Figure 4**).

During the green and black ripening stages (from August 11 to September 22), oleoside-11-methyl ester showed increases from 2.2 to 4.2 μmol/g to remain practically constant (3 μmol/g) until the end of the process. This fits with the oleuropein values that remained constant between 3 and 2 μmol/g (between August 28 and September 22, respectively). This fact allows us to disregard that oleoside-11-methyl ester is a degradation product of oleuropein by esterase activity.

Arbequina Variety. **Figure 4** shows that the presence of oleuropein precursors, oleoside-11-methyl ester, tyrosol, and ligstroside, was lower than that in the Hojiblanca variety, whereas the presence of oleuropein was higher. With regard to the major compounds, the presence of aglycone forms was also higher. Involvement of the precursors in oleuropein biosynthesis can be clearly appreciated in this variety. The decrease in the concentration from June 30 to July 28 for all precursors was devoted to maintain oleuropein levels at around 12 μmol/g. This concentration increased continuously until September 8, reaching a net synthesis that is 40 μmol/g greater than that shown in the Hojiblanca variety. The net increase in this period was 28 μmol/g, which represents 65%. The fact that there was a much lower level of

Table 2. Individual and Total Oleuropein and Ligstroside Aglycon Concentrations during the Fruit Vegetative Cycle of *O. europaea* L. Fruits (Hojiblanca and Arbequina cvs.)[a]

	concentration (μmol/g)					
	Hojiblanca			Arbequina		
harvest date	3,4-DHPEA-EA	*p*-DHPEA-EA	total	3,4-DHPEA-EA	*p*-DHPEA-EA	total
June 30	201.06 ± 10.27 a	45.04 ± 3.20 a	246.10 ± 12.46 a	196.41 ± 9.25 a	18.17 ± 1.36 b	214.58 ± 13.21 a
July 14	27.78 ± 1.77 c	22.23 ± 1.60 c	50.01 ± 3.18 b	45.51 ± 3.09 b	10.75 ± 0.78 d	56.26 ± 3.27 b
July 28	17.02 ± 1.01 e	17.59 ± 1.27 e	34.61 ± 2.10 c	40.18 ± 2.78 d	9.72 ± 0.73 f	49.91 ± 3.20 d
August 11	14.16 ± 0.82 g	14.38 ± 1.04 g	28.54 ± 1.79 e	38.28 ± 2.60 f	8.98 ± 0.67 h	47.26 ± 2.81 f
August 28	8.10 ± 0.52 i	14.22 ± 1.05 i	22.32 ± 1.46 g	15.18 ± 1.03 h	9.02 ± 0.68 j	24.21 ± 1.53 g
September 8	9.29 ± 0.56 k	14.04 ± 1.07 k	23.33 ± 1.51 h	15.51 ± 1.04 j	8.82 ± 0.63 l	24.33 ± 1.75 h
September 22	9.31 ± 0.55 m	14.74 ± 1.08 m	24.05 ± 1.60 i	12.71 ± 0.96 l	7.58 ± 0.55 n	20.29 ± 1.03 j
October 6	8.84 ± 0.49 o	14.36 ± 1.05 o	23.20 ± 1.39 k	5.41 ± 0.46 n	10.40 ± 0.79 p	15.81 ± 0.98 l
October 20	7.96 ± 0.43 q	13.95 ± 1.03 q	21.91 ± 1.06 m	1.41 ± 0.10 p	4.19 ± 0.31 r	5.60 ± 0.43 n
November 3	6.45 ± 0.38 s	13.45 ± 1.01 s	19.90 ± 0.98 o	1.06 ± 0.08 r	3.28 ± 0.24 t	4.34 ± 0.28 p
November 17	7.86 ± 0.41 u	11.20 ± 0.83 u	19.06 ± 0.89 q	0.58 ± 0.03 v	1.18 ± 0.09 v	1.77 ± 0.09 r
December 1	6.60 ± 0.36 x	4.20 ± 0.31 x	10.80 ± 0.76 s	0.26 ± 0.02 y	0.80 ± 0.06 y	1.06 ± 0.05 t
December 15	4.03 ± 0.28 w	2.40 ± 0.21 w	6.43 ± 0.58 u	0.07 ± 0.01 z	0.02 ± 0.01 z	0.09 ± 0.01 v

[a] Each value represents the mean ± RSD. Each value is the average based on two determinations. For the same component, values in different columns followed by different letters are significantly different (Tukey's multiple range test, where $p < 0.05$).

Table 3. Individual and Total Dialdehydic Oleuropein and Ligstroside Aglycon Concentrations during the Vegetative Cycle of *O. europaea* L. Fruits (Hojiblanca and Arbequina cvs.)[a]

	concentration (μmol/g)					
	Hojiblanca			Arbequina		
harvest date	3,4-DHPEA-EDA	*p*-DHPEA-EDA	total	3.4-DHPEA-EDA	*p*-DHPEA-EDA	total
June 30	227.97 ± 15.50 a	3.34 ± 0.24 a	231.31 ± 13.21 a	258.32 ± 16.79 a	1.16 ± 0.09 b	259.48 ± 14.25 a
July 14	78.05 ± 6.09 c	2.91 ± 0.21 c	80.96 ± 6.13 b	192.45 ± 12.09 b	0.73 ± 0.06 d	193.18 ± 12.45 c
July 28	39.50 ± 2.45 e	2.02 ± 0.15 e	41.52 ± 2.98 d	47.22 ± 2.83 d	1.33 ± 0.11 f	48.55 ± 3.01 e
August 11	9.23 ± 0.63 g	0.20 ± 0.01 g	9.43 ± 0.58 f	42.87 ± 2.74 f	0.21 ± 0.02 g	43.08 ± 2.89 g
August 28	4.63 ± 0.31 i	0.08 ± 0.01 h	4.71 ± 0.24 h	42.19 ± 2.74 h	0.16 ± 0.01 i	42.35 ± 2.15 i
September 8	3.38 ± 0.23 k	0.02 ± 0.01 j	3.40 ± 0.25 j	42.02 ± 2.73 j	0.01 ± 0.01 j	42.03 ± 2.12 k
September 22	2.96 ± 0.20 m	0.01 ± 0.01 k	2.97 ± 0.19 l	40.21 ± 2.65 l	0.02 ± 0.01 k	40.23 ± 1.98 m
October 6	2.72 ± 0.18 o	0.01 ± 0.01 l	2.73 ± 0.15 n	25.99 ± 1.74 n	0.23 ± 0.01 m	26.22 ± 1.78 o
October 20	1.65 ± 0.11 q	0.02 ± 0.01 n	1.67 ± 0.10 p	26.96 ± 1.83 p	0.41 ± 0.03 o	27.37 ± 1.81 q
November 3	1.04 ± 0.07 s	0.01 ± 0.01 p	1.05 ± 0.09 r	25.16 ± 1.71 r	0.44 ± 0.03 q	25.60 ± 1.67 s
November 17	0.76 ± 0.05 u	0.01 ± 0.01 s	0.77 ± 0.03 t	32.32 ± 2.20 t	0.47 ± 0.04 r	32.79 ± 2.03 u
December 1	0.75 ± 0.06 y	0.00 u	0.75 ± 0.03 x	30.93 ± 2.13 v	0.81 ± 0.05 t	31.74 ± 2.01 y
December 15	0.74 ± 0.06 z	0.00 x	0.74 ± 0.03 w	31.58 ± 2.17 w	0.06 ± 0.01 v	31.64 ± 1.92 z

[a] Each value represents the mean ± RSD. Each value is the average based on two determinations. For the same component, values in different columns followed by different letters are significantly different (Tukey's multiple range test, where $p < 0.05$).

precursors than those shown for Hojiblanca indicates that the precursors were metabolized in the Arbequina variety much more quickly than in the Hojiblanca variety.

The elenolic acid variation profile differs from that shown by Hojiblanca, showing two maxima. The first maximum, 14.6 μmol/g, appeared on August 11, with a net increase of 9.4 μmol/g compared to July 28, which agrees with the oleuropein accumulation, which changed from 12.0 to 20 μmol/g, with a net increase of 8 μmol/g. This increase is influenced by the β-glucosidase activity, which would degrade oleoside-11-methyl ester (**Figure 5**). The fact that the decrease in oleoside-11-methyl ester content took place in parallel to the increase of the elenolic acid supports the hypothesis that elenolic acid comes directly from the precursor oleoside-11-methyl ester via enzymatic activity of β-glucosidase. However, the second maximum (October 6) matches with the sharp decrease of oleuropein from 40 to 11 μmol/g, with a net loss of 29 μmol/g, observed between September 8 and October 6. This decrease could be due to the combined action of esterase and β-glucosidase activities on oleuropein that produces oleoside-11-methyl ester and elenolic acid, respectively (**Figure 5**).

Levels of precursors, oleoside-11-methyl ester, tyrosol, and ligstroside, decreased until August 28 and then increased at the evaluation on September 8, which overlaps with the maximum content on oleuropein. The mass balance of tyrosol reflects either increases or losses: from 2.4 to 0.8 μmol/g between June 30 and July 28, from 0.8 to 0.1 μmol/g between July 28 and August 11, and from 1.0 to 0.2 μmol/g between August 11 and September 8. Additionally, an increase in the ligstroside content was denoted (from 0.8 to 4.6 μmol/g between August 28 and September 8). This shows that the metabolic pathway is active, resulting in an increase in oleuropein from 12.0 to 20 μmol/g, from 20 to 28.6 μmol/g, and from 28.6 to 40 μmol/g (**Figure 4**). In this variety, the esterification of 7-β-1-D-glucopyranosyl-11-methyl oleoside with tyrosol to form ligstroside was fast. This fact impaired an appropriate monitoring of this precursor (**Figure 4**). Consequently, the absolute value detected for tyrosol is lower than that for Hojiblanca, but its role in the oleuropein pathway is greater.

In a similar fashion to the Hojiblanca variety, oleuropein aglycone and 3,4-DHPEA-EDA content started with higher concentration values than the rest of the phenols monitored in this study (196.4 and 258.3 μmol/g, respectively; **Tables 2** and **3**), indicating that the catabolic pathway is greater than the anabolic pathway. **Figure 6B** shows the changes in β-glucosidase activity, which reached a maximum value that is twice than that for Hojiblanca. The high activity of this enzyme produced a continuous and greater presence of 3,4-DHPEA-EDA, with a significantly higher content in the Arbequina variety throughout the different ripening stages.

Similarly, the total amounts of oleuropein and ligstroside aglycones (**Table 2**) were significantly higher in the Arbequina variety (except in the first sampling) until September 8 because of high enzymatic activity of β-glucosidase in this variety. The same applied to 3,4-DHPEA-EDA (**Table 3**), which showed statistically higher absolute values in the Arbequina variety throughout the complete study, according to the high β-glucosidase activity (**Figure 6B**). This fact supports that 3,4-DHPEA-EA is the preferred substrate in this variety for the consecutive reactions that produce 3,4-DHPEA-EDA, probably because the enzymatic systems are more active in the Arbequina variety.

From August 11, the oleuropein aglycone 3,4-DHPEA-EA (**Table 2**) undergoes a marked decline, while 3,4-DHPEA-EDA (**Table 3**) decreases very gradually. The transformation of ligstroside into its aglycone, *p*-HPEA-EA, is fast and presents higher values than its predecessor, while the formation of *p*-HPEA-EDA is slower, unlike that of 3,4-DHPEA-EDA. During the rest of the green and black ripening, arbitrary increases and decreases were observed without any specific pattern. The increase in *p*-HPEA-EDA may be derived from ligstroside aglycone between sampling 6 and 10. The final increase in oleuropein is analogous to another increase in oleoside-11-methyl ester and *p*-HPEA-EDA, which can only be explained by rearrangements or transport mechanisms that mobilize substrates among various locations in the plant (*26*). On this subject, Parr and Bolwell (*27*) address the transport and metabolic compartmentalization systems implicated in the movement of phenolic substrates, which are not yet fully understood. The fact that the olive tree blooms several times consecutively could affect and explain the results obtained.

Finally, it is important to point out that this is the first study analyzing the evolution of the precursors of oleuropein, oleoside-11-methyl ester, tyrosol, and ligstroside, and the enzymatic degradation products, elenolic acid and the aglycone forms of oleuropein and ligstroside, during the vegetative cycle of *O. europaea* fruits. The results support that the oleuropein biosynthesis follows the pathway proposed by Damtoft et al. (*12*) in Hojiblanca and Arbequina varieties. In addition, the high activity

of β-glucosidase found in both varieties acting directly on glycosilated phenols produces a modulation of the *in vivo* synthesis of oleuropein and its precursors, confirming that this enzyme diminishes the accumulation of oleuropein, which is the major compound in a wide range of olive varieties. The enzymatic activity produces elenolic acid and the aglycone forms of oleuropein and ligstroside as the main degradation products. It is worth mentioning that this complex metabolic process of oleuropein varies depending upon the variety, with the Arbequina variety showing active metabolic routes sustained in time and with better yields than the Hojiblanca variety. Considering that climate and agronomic conditions effect the polyphenolic content of olive fruits, further studies are required to confirm this working hypothesis.

ACKNOWLEDGMENT

We thank Visitación Ortega Márquez and Sergio Alcañiz García for technical assistance and the Agricultural Experimental Station of Cabra (Córdoba, Spain) for supplying the olive fruits. Professor María Isabel Mínguez-Mosquera is retired after 50 years intensely devoted to science.

LITERATURE CITED

(1) Amiot, M. J.; Fleuriet, A.; Macheix, J. J. Accumulation of oleuropein derivates during olive maturation. *Phytochemistry* **1989**, *28*, 67−69.

(2) Amiot, M. J.; Fleuriet, A.; Macheix, J. J. Importance and evolution of phenolic compounds in olive during growth and maturation. *J. Agric. Food Chem.* **1986**, *34*, 823−826.

(3) Limiroli, R.; Consonni, R.; Ranalli, A.; Bianchi, G.; Zetta, L. ^{1}H-NMR study of phenolics in the vegetation water of three cultivars of *Olea europaea*: Similarities and differences. *J. Agric. Food Chem.* **1996**, *44*, 2040−2048.

(4) Esti, M.; Cinquanta, L.; La Notte, E. Phenolic compounds in different olive varieties. *J. Agric. Food Chem.* **1998**, *46*, 32−35.

(5) Ryan, D.; Antolovich, M.; Prenzler, P.; Robards, K.; Lavee, S. Biotransformations of phenolic compounds in *Olea europaea* L. *Sci. Hortic.* (*Amsterdam, Neth.*) **2002**, *92*, 147−176.

(6) Ranalli, A.; Marchegiani, D.; Contento, S.; Girardi, F.; Nicolosi, M. P.; Brullo, M. D. Variations of iridoid oleuropein in Italian olive varieties during growth and maturation. *Eur. J. Lipid Sci. Technol.* **2009**, *111*, 678−687.

(7) Morelló, J. R.; Romero, M. P.; Motilva, M. J. Effect of the maturation process of the olive fruit on the phenolic fraction of drupes and oils from Arbequina, Farga, and Morruts cultivars. *J. Agric. Food. Chem.* **2004**, *52*, 6002−6009.

(8) Ryan, D.; Prenzler, P.; Lavee, S.; Antolovich, M.; Robards, K. Quantitative changes in phenolic content during physiological development of the olive (*Olea europaea*) cultivar Hardy's Mammoth. *J. Agric. Food Chem.* **2003**, *51*, 2532−2538.

(9) Ryan, D.; Antolovich, M.; Herlt, T.; Prenzler, P. D.; Lavee, S.; Robards, K. Identification of phenolic compounds in tissues of the novel olive cultivar Hardy's Mammoth. *J. Agric. Food Chem.* **2002**, *50*, 6716−6724.

(10) Inouye, H.; Ueda, S.; Inoue, K.; Takeda, Y. Biosynthesis of oleuropein-type secoiridoid glucosides by oleaceae. *Tetrahedron Lett.* **1971**, *43*, 4073−4076.

(11) Inouye, H.; Ueda, S.; Inoue, K.; Takeda, Y. Studies on monoterpene glucosides and related natural products. XXIII. Biosynthesis of the secoiridoid glucosides, gentiopicroside, morroniside, oleuropein and jasminin. *Chem. Pharm. Bull.* **1974**, *22*, 676−686.

(12) Damtoft, S.; Franzyk, H.; Jensen, S. R. Biosynthesis of secoiricoid glucosides in Oleaceae. *Phytochemistry* **1993**, *34*, 1291−1299.

(13) Damtoft, S.; Franzyk, H.; Jensen, S. R. Biosynthesis of iridoids in Syringa and Fraxinus: Secoiridoid precursors. *Phytochemistry* **1995**, *40*, 773−784.

(14) Damtoft, S.; Franzyk, H.; Jensen, S. R. Biosynthesis of iridoids in Syringa and Fraxinus: Carbocyclic iridoid precursors. *Phytochemistry* **1995**, *40*, 785−792.

(15) Pérez, J. A.; Hernández, J. M.; Trujillo, J. M.; López, H. Iridoids and secoiridoids from Oleaceae. In *Studies in Natural Products Chemistry*; Rahman, A., Ed.; Elsevier: Amsterdam, The Netherlands, **2005**; Vol. *32*, Part 12, pp 303−368.

(16) Soler-Rivas, C.; Espín, J. C.; Wichers, H. J. Oleuropein and related compounds. *J. Sci. Food Agric.* **2000**, *80*, 1013−1023.

(17) Artajo, L. S.; Romero, M. P.; Morelló, J. R.; Motilva, M. P. Enrichment of refined olive oil with phenolic compounds: Evaluation of their antioxidant activity and their affect on the bitter index. *J. Agric. Food Chem.* **2006**, *54*, 6079−6088.

(18) Ríos-Martin, J. J.; Gutiérrez-Rosales, F. Comparison of methods extracting phenolic compounds from lyophilised and fresh olive pulp. *LWT—Food Sci. Technol.* **2010**, *43*, 1285−1288.

(19) Suárez, M.; Macià, A.; Romero, M. P.; Motilva, M. J. Improved liquid chromatography tandem mass spectrometry method for the determination of phenolic compounds in virgin olive oil. *J. Chromatogr., A* **2008**, *1214*, 90−99.

(20) Romero-Segura, C.; Sanz, C.; Pérez, A. G. Purification and characterization of an olive fruit β-glucosidase involved in the biosynthesis of virgin olive oil phenolics. *J. Agric. Food Chem.* **2009**, *57*, 7983−7988.

(21) Minguez-Mosquera, M. I.; Gandul-Rojas, B.; Gallardo-Guerrero, L. Measurement of chlorophyllase activity in olive fruit (*Olea europaea*). *J. Biochem.* **1994**, *116*, 263−268.

(22) Capasso, R.; Evidente, A.; Visca, C.; Gianfreda, L.; Maremonti, M.; Greco, G., Jr. Production of glucose and bioactive aglycone by chemical and enzymatic hydrolisis of purified oleuropein from *Olea europea*. *Appl. Biochem. Biotechnol.* **1996**, *61*, 365−377.

(23) Obied, H. K.; Bedgood, D. R.; Prenzler, P. D.; Robards, K. Chemical screening of olive biophenol extracts by hyphenated liquid chromatography. *Anal. Chim. Acta* **2007**, *603*, 176−189.

(24) Vierhuis, E.; Servili, M.; Baldioli, M.; Schols, H. A.; Voragen, A. G. J.; Montedoro, G. F. Effect of enzyme treatment during mechanical extraction of olive oil on phenolic compounds and polysaccharides. *J. Agric. Food Chem.* **2001**, *49*, 1218−1223.

(25) Montedoro, G.; Servili, M.; Baldioli, M.; Selvaggini, R.; Miniati, E.; Macchioni, A. Simple and hydrolyzable compounds in virgin olive oil. 3. Spectroscopic characterizations of the secoiridoid derivatives. *J. Agric. Food Chem.* **1993**, *41*, 2228−2234.

(26) Fernández-Bolaños, J.; Rodríguez, R.; Guillén, R.; Jiménez, A.; Heredia, A. Activity of cell wall-associated enzymes in ripening olive fruit. *Physiol. Plant.* **1995**, *93*, 651−658.

(27) Parr, A. J.; Bolwell, G. P. Phenols in the plant and in man. The potential for possible nutritional enhancement of the diet by modifying the phenols content or profile. *J. Sci. Food Agric.* **2000**, *80*, 985−1012.

Received for review August 9, 2010. Revised manuscript received November 10, 2010. Accepted November 12, 2010. This study was possible by the financial support of the Ministerio de Ciencia e Innovación (Spanish Government, AGL2007-66139-C02).